

# Discontinuous Dielectrophoresis

## *A Technique for Investigating the Response of Loosely Adherent Cells to High Shear Stress*

Rebecca Soffe<sup>1</sup>, Sara Baratchi<sup>2</sup>, Shi-yang Tang<sup>1</sup>, Peter McIntyre<sup>2</sup>,  
Arnan Mitchell<sup>1</sup> and Khashayar Khoshmanesh<sup>1</sup>

<sup>1</sup>*School of Electrical and Computer Engineering, RMIT University, 124 La Trobe St., Melbourne, Australia*

<sup>2</sup>*Health Innovations Research Institute and School of Medical Sciences, RMIT University, Plenty Rd., Melbourne, Australia*

**Keywords:** Discontinuous Dielectrophoresis, Dielectrophoresis, Microfluidics, Shear-Induced Stress, Intracellular Calcium Signalling, HEK-293.

**Abstract:** The functioning of cells under mechanical stress influences several cellular processes, for example proliferation, organogenesis, and transcription. Current techniques used to examine mechanical stress on loosely adherent cells, are however, primarily focused on single individual cells being stimulated, or require time-consuming surface coating techniques; and are limited in the level of shear stress that can be supplied to immobilised cells. Here we report the process of the technique, discontinuous dielectrophoresis; which enables high shear stress analysis of clusters of immobilised loosely adherent cells, we have analysed the performance of the system using *Saccharomyces cerevisiae* yeast cells, up to a shear stress of 42 dyn/cm<sup>2</sup>. Additionally, we provide application experimental results from investigating shear induced calcium signalling of HEK-293-TRPV4 cells at flow rates of 2.5, and 120 µl/min, corresponding to shear stress levels of 0.875 and 42 dyn/cm<sup>2</sup>, respectively. In summary, discontinuous dielectrophoresis will enable the investigation of the mechanotransduction behaviour of loosely adherent cells under physiologically relevant shear stresses. Additionally, discontinuous dielectrophoresis provides the capability for parallelism, and dynamic control over the microenvironment, as previously explored by different microfluidic platforms without the capacity for high shear stress analysis of loosely adherent cells.

## 1 INTRODUCTION

Our technique differs from existing permanent immobilisation techniques, as it enables loosely adherent cells to be investigated under shear stress magnitudes higher than previously reported (Mendoza et al., 2010, Yamamoto and Ando, 2013).

Various conventional techniques either on-chip or off-chip are used to immobilise both adherent and non-adherent cells, to carry out various biological assays and microscopy techniques, in the absence of shear stress. Furthermore, predominantly conventional methods are focused on surface modification techniques, which include for example, ligands, biometric peptides, and cell adhesive peptides. Such techniques do not facilitate the robust immobilisation required for applying high shear stress, to loosely adherent cells; potentially as some systems are not intentionally designed for high shear stress analysis (Mutreja et al., 2015, El-Ali et al.,

2006, Nahavandi et al., 2014, Berthier et al., 2012, Yamamoto and Ando, 2013, Baratchi et al., 2014, Voldman, 2006). However, Baratchi et al. utilised surface modification techniques on a microfluidic platform to apply shear stress, however this was limited to the lower end of the physiological shear stress range (Baratchi et al., 2014).

Moreover, microfluidic-based immobilisation techniques such as dielectrophoresis, magnetophoresis, or acoustophoresis, require the electric, magnetic, or acoustic field, be active throughout the duration of the experimentation to keep cells immobilised, and often limited to low shear stress levels to avoid dislodgement of cells (Soffe et al., 2015b, Ding et al., 2012, Voldman, 2006). In contrast, in our technique the electric field is activated for just 120 seconds, which in turn minimizes the negative impact on cells and simplifies the experimental procedure (Soffe et al., 2015a).

Although permanent immobilisation of proteins by means of dielectrophoresis has been previously demonstrated by T. Yamamoto, et al. (Yamamoto and Fujii, 2007), our technique differs from their work, as it enables the permanent immobilisation of multiple cells rather than small clusters of proteins; additionally, and more importantly our technique enables the patterned cells to remain attached to the surface even at high shear stress levels.

## 2 DISCONTINUOUS DIELECTROPHORESIS

Discontinuous dielectrophoresis is a technique based on dielectrophoresis; however, the application of the electric field is minimised, and high flow rates producing a shear stress over a cluster of cells can be achieved (Soffe et al., 2015a). Discontinuous dielectrophoresis overcomes limitations of dielectrophoresis, as previously mentioned, regarding the reduced activation period of the electric field and the ability to conduct experiments in biologically relevant suspension media, due to the deactivation of the electric field. Furthermore, immobilised cells are able to withstand high levels of shear stress; here we report experiments using shear stress levels up to 42 dyn/cm<sup>2</sup>.

In this section we give a brief overview of the theory of dielectrophoresis, the design of the microfluidic platform used to develop discontinuous dielectrophoresis, the procedure of discontinuous dielectrophoresis, and analysis of the discontinuous dielectrophoresis, in terms of trapping efficiency of immobilised cells. Taking note, that *Saccharomyces cerevisiae* yeast cells are used as our model cell, which is commonly used to show proof of concept technologies and known to be non-adherent.

### 2.1 Dielectrophoresis Overview

Dielectrophoresis is a phenomenon, in which a non-uniform electric field is used to induce motion into polarisable particles; consequently, label-free manipulation can be achieved. Currently dielectrophoresis systems have been demonstrated for the manipulation, sorting, immobilisation, and characterisation of a variety of bio-particles.

The response of a particle in an electric field is governed by the dielectric properties, such as structural, morphological, and chemical characteristics. Furthermore, the time average dielectrophoretic force ( $\langle F_{DEP} \rangle$ ) experienced on a

spherical particle developed by Morgan and Green, is governed by the following equation (Morgan and Green, 2003, Chapter 4):

$$\langle F_{DEP} \rangle = 2\pi r^3 \epsilon_{cell} \epsilon_0 \epsilon_{med} \text{Re}\{f_{CM}\} \nabla |E_{rms}|^2 \quad (1)$$

Where  $r$  is the radius of the cell,  $\epsilon_0$  and  $\epsilon_{med}$ , are the permittivity of free space ( $8.854 \times 10^{-12}$  F/m) and the suspension medium, respectively; in addition  $\text{Re}\{f_{CM}\}$ , is the real component of the Clausius-Mossotti factor, and  $E_{rms}$ , is the electric field root-mean-squared. A more extensive analysis is presented in the succeeding subsection, for the electric field, and dielectrophoretic force induced by the interdigital microelectrodes.

The Clausius-Mossotti factor ( $f_{CM}$ ) for a homogenous spherical structure is given by (Morgan and Green, 2003, Chapter 3):

$$f_{CM} = \frac{\epsilon_{cell}^* - \epsilon_{med}^*}{\epsilon_{cell}^* + 2\epsilon_{med}^*}, \quad (2)$$

where, complex permittivity,  $\epsilon^*$ , is given by:

$$\epsilon^* = \epsilon - \frac{i\sigma}{\omega}, i = \sqrt{-1}, \quad (3)$$

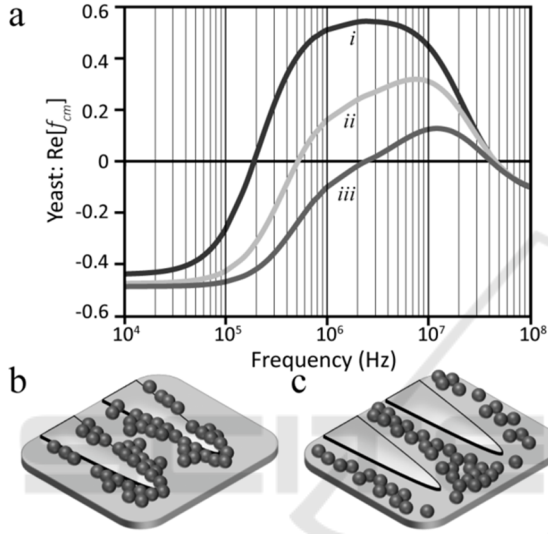
where,  $\epsilon_{cell}^*$  and  $\epsilon_{med}^*$ , are the complex permittivities of the cell and suspension medium, respectively; in addition,  $\sigma$ , is the electrical conductivity, and  $\omega$ , is the angular frequency of the applied signal. The real part of the complex variable Clausius-Mossotti factor, provides an indication of the behaviour of a particle within the electric field at various medium.

Furthermore, this behaviour is presented in **Figure 1a** for three different medium conductivities (200, 500, 1000  $\mu\text{S/cm}$ ) over a frequency range of  $10^4$  to  $10^8$  Hz, calculated with the geometric and dielectric properties for the *Saccharomyces cerevisiae* yeast cell as given in **Table 1**. The cells were suspended in an isotonic low electrical conductivity (LEC, 8.5% w/v sucrose, 0.3% dextrose,  $\sim 100 \mu\text{S/cm}$ ) buffer, with the conductivity adjusted with the addition of phosphate-buffered saline (PBS). Such that when the real component of the Clausius-Mossotti factor is positive, the cells are attracted to the microelectrodes, a phenomenon that is commonly known as positive dielectrophoresis (**Figure 1b**). On the other hand, when the real component of Clausius-Mossotti factor is negative, the cells are repelled from the microelectrodes; a phenomenon more commonly known as negative dielectrophoresis (**Figure 1b**).

The Clausius-Mossotti factor response (**Figure 1**) is heavily influenced by the complex permittivity of the cell ( $\epsilon_{cell}^*$ ). In our case we are using a yeast cell, which has a cell wall, thus, a two shell model

Table 1: Geometric and dielectric properties of viable yeast cells (Urdaneta and Smela, 2007).

Parameter	Value
Cell diameter	8 $\mu\text{m}$
Membrane thickness	8 nm
Wall thickness	220 nm
Cytoplasm conductivity	0.2 S/m
Cytoplasm permittivity	$50\epsilon_0$ F/m
Membrane conductivity	$25\epsilon_0$ S/m
Membrane permittivity	$6\epsilon_0$ F/m
Wall conductivity	$14\epsilon_0$ S/m
Wall permittivity	$60\epsilon_0$ F/m


 Figure 1: (a) The real part of Clausius-Mossotti factor response to frequency for yeast cells at medium conductivities of (i) 200, (ii) 500, and (iii) 1000  $\mu\text{S/cm}$ , for cells suspended in LEC, with conductivities adjusted with PBS. Schematic representation of: (b) positive, and (c) negative dielectrophoresis.

encompassing the geometric and dielectric properties of the yeast cells given in **Table 1**, which is given by (Huang et al., 1992):

$$\begin{aligned} \epsilon_{cyto-mem}^* &= \epsilon_{mem}^* \frac{\left[\frac{r_{mem}}{r_{cyto}}\right]^3 + 2 \left[\frac{\epsilon_{cyto}^* - \epsilon_{mem}^*}{\epsilon_{cyto}^* + 2\epsilon_{mem}^*}\right]}{\left[\frac{r_{mem}}{r_{cyto}}\right]^3 - \left[\frac{\epsilon_{cyto}^* - \epsilon_{mem}^*}{\epsilon_{cyto}^* + 2\epsilon_{mem}^*}\right]}, \quad (4) \end{aligned}$$

$$\begin{aligned} \epsilon_{cell}^* &= \epsilon_{wall}^* \frac{\left[\frac{r_{cell}}{r_{mem}}\right]^3 + 2 \left[\frac{\epsilon_{cyto-mem}^* - \epsilon_{wall}^*}{\epsilon_{cyto-mem}^* + 2\epsilon_{wall}^*}\right]}{\left[\frac{r_{cell}}{r_{mem}}\right]^3 - \left[\frac{\epsilon_{cyto-mem}^* - \epsilon_{wall}^*}{\epsilon_{cyto-mem}^* + 2\epsilon_{wall}^*}\right]}. \quad (5) \end{aligned}$$

Where,  $\epsilon_{cyto}^*$ ,  $\epsilon_{mem}^*$ ,  $\epsilon_{wall}^*$ , and  $\epsilon_{cyto-mem}^*$  are the complex permittivities of the cell cytoplasm, membrane, wall, and the equivalent combined

homogenous cell cytoplasm and membrane, respectively.

## 2.2 Dielectrophoresis Platform Design

The microfluidic platform consists of two main components, the microelectrodes and the microchannel; both are designed to facilitate the maximum immobilised cell population visible when using microscopy techniques (**Figure 2**). In the following subsections the design and fabrication procedure will be outlined; including, the analysis of the resulting electric field and shear stress contours produced through the microfluidic channel, when applying a flow rate between 0 and 120  $\mu\text{l/min}$ , corresponding to a shear stress range from 0 to 42  $\text{dyn/cm}^2$ .

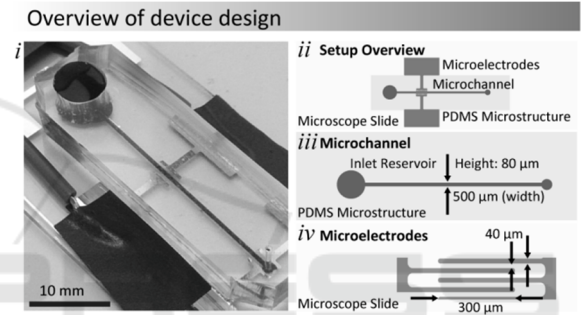


Figure 2: (a) Overview of the device design: (i) Photograph of the microfluidic platform; schematic with corresponding relevant dimensions of features of: (ii) Plan view of the setup overview; (iii) Microchannel; and (iv) Microelectrodes.

### 2.2.1 Microelectrode Design and Fabrication

To maximise the uniformity of the patterning of immobilised cells an interdigital microelectrode design was invoked, as presented in **Figure 2**. Consequently, this maximised the cell population immobilised within microscopic imaging range, under a  $10\times$  objective (with a  $1.5\times$  multiplier) on a Nikon Eclipse (TE 2000). The microelectrodes were designed to have a gap and width of  $40\ \mu\text{m}$ , which is the smallest possible feature resolution available to us to fabrication limitations. Furthermore, the active region was designed to be  $300\ \mu\text{m}$ , such that spanning the entire imaging range.

The microelectrodes were fabricated in two stages. Initially the thin films were fabricated using evaporation on a glass microscope slide, using a gold on chrome process, at thickness of 1500 and  $500\ \text{\AA}$ , respectively. The microelectrodes were then patterned using standard microfabrication

techniques, including photolithography and wet etching (Nasabi et al., 2013).

### 2.2.2 Electric Field Analysis

To determine the influence of the electric field on the time averaged dielectrophoretic force experienced on a spherical cell, the electric field contours are determined (**Figure 3**). Laplace equations are solved within the microfluidic channel (design presented in succeeding subsection), through applying electric potentials accordingly, to determine the electric field contours.

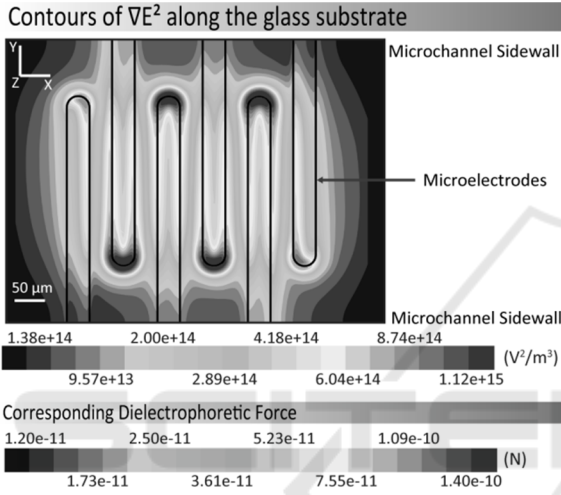


Figure 3: (a) Contours of the gradient of the square of the electric field ( $E$ ,  $V^2/m^3$ ) and corresponding dielectrophoretic force ( $\langle F_{DEP} \rangle$ , N).

Using the general rule of thumb that there is zero electric flux along the surfaces of the microchannel, other than the glass substrate (microscope slide) where the microelectrodes are fabricated; thus, flux is zero along the sidewalls and top of the microchannel. Thus, resulting in a flux relationship given as:

$$\nabla^2 \phi_{rms} = 0. \quad (6)$$

Additionally, the electric field strength ( $E$ ) is determined by taking the gradient of the electric potential ( $\phi$ ), resulting in the following relationship:

$$E = -\nabla \phi_{rms}. \quad (7)$$

Furthermore, as seen in **Equation 1** the time average dielectrophoretic force is proportional to the electric field strength as given by (**Figure 3**):

$$\langle F_{DEP} \rangle \propto \nabla E^2, \quad (8)$$

Simulations indicated the maximum force experienced on the cells was  $1.40e^{-10}$  N (**Figure 3**).

### 2.2.3 Microchannel Design and Fabrication

Microchannel was designed to encompass the width of the active electric field, being  $300 \mu m$  (**Figure 2**). Consequently, the width of the microchannel was designed to have a width of  $500 \mu m$ , to ensure that the strongest section of the electric field (tip region of the microelectrodes) was not within the imaging region. Furthermore, the channel was designed to have an arbitrary height of  $80 \mu m$ , which allowed cells to immobilise along the microelectrodes, and cells and suspension to wash over the immobilised cells without dislodging them.

The polydimethylsiloxane (PDMS) microchannel ( $500 \times 80 \mu m$ ) was fabricated using standard soft lithography and replica molding techniques (Whitesides et al., 2001). The PDMS was cured using a standard ratio of Sylgard 184, with the base to curing agent ratio 10:1 (Dow Corning Corporation, MI).

### 2.2.4 Velocity and Shear Stress Profiles

In order to determine the shear stress being applied to the immobilised cells on the microelectrodes, computational fluidic dynamic simulations were carried out (**Figure 4**).

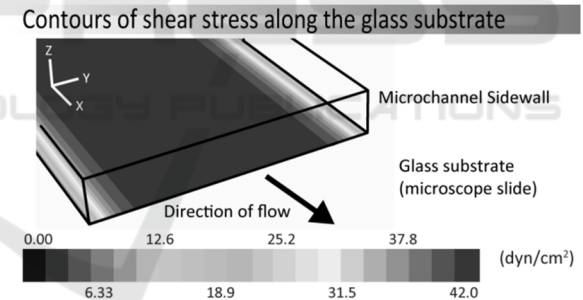


Figure 4: Contours of the shear stress across the substrate.

Given that the flow is laminar and the liquid is assumed to be Newtonian the following equations apply. The continuity equation is given by:

$$\nabla \cdot \mathbf{U} = 0. \quad (8)$$

Furthermore the momentum of the liquid is given by:

$$\rho_{liquid}(\mathbf{U} \cdot \nabla)\mathbf{U} = -\nabla P + \mu_{liquid}\nabla^2\mathbf{U}. \quad (9)$$

Where,  $\mathbf{U}$ ,  $P$ ,  $\rho_{liquid}$ , and  $\mu_{liquid}$ , are velocity, pressure, density, and dynamic viscosity of the liquid, respectively. Note that the assumed boundary conditions of ambient pressure at the inlet, desired flow rate through entire microchannel, and no-slip at the sidewalls is used to evaluate these equations. To determine the shear stress over the glass substrate (microscope slide), one assumes that the

immobilised cells do not influence the hydrodynamic properties of the cells; thus, the resulting shear stress ( $\tau$ ) is given by:

$$\tau|_{glass\_sub} = \mu_{liquid} \left. \frac{\partial U}{\partial z} \right|_{z=0}. \quad (10)$$

Furthermore, the resulting shear stress profiles can be determined along the glass substrate; such as presented in **Figure 4** for a flow rate of 120  $\mu\text{l}/\text{min}$ , corresponding to a shear stress of 42  $\text{dyn}/\text{cm}^2$ . The relationship of flow rate ( $Q$ ) and shear stress for our microfluidic platform is given by:

$$\tau = \frac{67.5 \mu_{liquid} Q}{WH^2}, \quad (11)$$

where,  $W$  and  $H$ , are the width and height of the microchannel. Additionally, the relationship drag force exerted on a cell is given by is given by:

$$\text{Drag} = 4\pi r_{cell} \tau. \quad (12)$$

The maximum reported flow rate of 120  $\mu\text{l}/\text{min}$ , corresponds to a drag force of  $8.40 \times 10^{-10}$  N.

## 2.3 Discontinuous Dielectrophoresis Procedure

The procedure required for discontinuous dielectrophoresis, is systematic; however, in some cases slightly different tactics need to be used, such as when using stains that are sensitive to shear stress. The fundamental discontinuous dielectrophoresis procedure is presented in **Figure 5** and each stage will be discussed in detail in the subsections.

### 2.3.1 Sample Preparation and Application

Samples need to be suspended in an isotonic low electrical conductivity (LEC) buffer, composed of 8.5% w/v sucrose, and 0.3% dextrose in deionised water; ensuring that the final suspension conductivity is 200  $\mu\text{S}/\text{cm}$ . In necessary, the solution conductivity can be increased through the addition of phosphate-buffered saline, or any other relevant biological buffer. The cell suspension is then transpired to the inlet reservoir of the microfluidic platform at a flow rate of 2.5  $\mu\text{l}/\text{min}$  (**Figure 2**). A low flow rate is used to ensure that cells can be immobilised once the electric field is activated. Additionally, this is advantageous when doing high shear stress analysis, as this minimises the pre-exposure to shear stress. In the case for yeast cells for a 100 ml volume, we added 20 mg of dried *S. cerevisiae* yeast cells (Sigma-Aldrich).

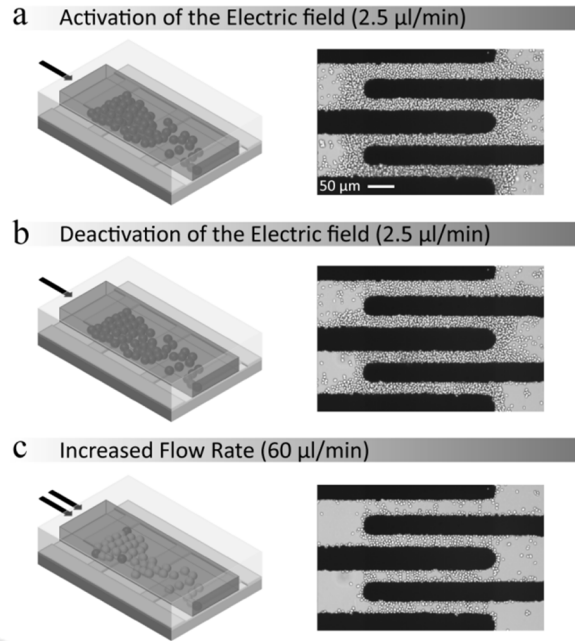


Figure 5: Schematic representation of procedure used for the discontinuous dielectrophoresis strategy: (a) Activation of the electric field for 120 s, excited by a 10 MHz 5  $V_{\text{pk-pk}}$  sinusoid, to immobilise the cells along the microelectrodes; with the cell suspension flown over the microelectrodes at a flow rate of 2.5  $\mu\text{l}/\text{min}$ ; (b) Deactivation of the electric field after 120 s of activation, with the flow rate remaining consistent; (c) Once cells have stabilised on the surface and reached equilibrium the flow rate can be increased to the desired flow rate, such as 60  $\mu\text{l}/\text{min}$ .

### 2.3.2 Activation of the Electric Field

Once cells are consistently flowing over the microelectrodes, the microelectrodes are activated, through the application of a 10 MHz sinusoid operating at 5  $V_{\text{pk-pk}}$ . The microelectrodes are kept active for a period of 120 s (**Figure 5a**). This was to minimise the duration of the electric field, thus minimising any harmful effects on the cells due to being within an electric field. Furthermore, the cell population can be controlled by an increase in the activation duration of the electric field; however, we recommend increasing the initial cell population.

The dielectrophoretic and shear forces on the cell influence the capacity of the cell to remain immobilised to the substrate. Such that the cells are immobilised using a flow rate of 2.5  $\mu\text{l}/\text{min}$ , which corresponds to a shear stress of 0.875  $\text{dyn}/\text{cm}^2$ , resulting in a drag force of  $1.77 \times 10^{-11}$  N being exerted on the cells. However, the force dielectrophoretic force exerted on the cells is determined to be  $1.40 \times 10^{-10}$  N (**Figure 3**). Consequently, as the

dielectrophoretic force is greater than the drag force generated, the cells are immobilised on the substrate; rather than being washing directly over the electrode in the event of a higher flow rate, which produces a greater shear stress and subsequent force.

### 2.3.3 Deactivation of the Electric Field

Once the field has been active for 120 s, the electric field is turned off. Deactivation of the electric field, resulted in the additional layers of cells and cells not correctly immobilised in the first layer being dislodged and washed away. Consequently, a single layer of immobilised cells remained, in the imaging range (**Figure 5b**). In general, it was observed that non-viable cells would not initially immobilise or was dislodged with increasing flow rate. Once the electric field is deactivated, the cell suspension can be exchanged to a suitable biological imaging media, in our case we exchanged for HEPES. The cells were then left for five minutes to stabilise in their immobilised location and reach equilibrium, especially in the occurrence that the media was exchanged to a biologically relevant media. Once these criteria were met, the flow rate was increased to the desired flow rate and resulting shear stress, as presented in **Figure 5c** for 60  $\mu\text{l}/\text{min}$ .

Furthermore once the electric field is inactivated, the dielectrophoretic force no longer influences the forces experienced on the cell. In the event the flow rate is increased to 120  $\mu\text{l}/\text{min}$ , corresponding to a drag force of  $8.40 \times 10^{-10}$  N. This force is considerably larger than the maximum dielectrophoretic force, demonstrating the adhesive attraction between the cell surface and the glass substrate produced during the discontinuous dielectrophoresis procedure.

### 2.3.4 Yeast Trapping Efficiency

To analyse the effectiveness of discontinuous dielectrophoresis, we investigated the trapping efficiency. Initially the cells are immobilised using the aforementioned procedure, then the flow rate of the system is increased sequentially in three minute intervals, at various flow rates between 2.5 and 100  $\mu\text{l}/\text{min}$ . Trapping efficiency was evaluated as:

$$\eta_{\text{trapping}} = \frac{n_{\text{remaining\_cells}}}{n_{\text{initial}}} \cdot 100\%, \quad (13)$$

where,  $n_{\text{remaining\_cells}}$ , and  $n_{\text{initial}}$  are the number of remaining and initial cell counts of immobilised viable cells.

Analysis of the trapping efficiency of yeast cells was carried out using three different exciting waveform voltages, when supplying the electric field

for the 120 s duration. The three selected voltages selected where 2.5, 5, and 10  $V_{\text{pk-pk}}$ , as presented in **Figure 6a** for cells suspended in LEC. Additional analysis was carried out using the optimal voltage of 5  $V_{\text{pk-pk}}$ , in which the suspension media was exchanged for HEPES after deactivation of the electric field. For the scenario that the cells were kept in LEC, the change in voltage provided no significant change in the trapping efficiency which was determined to be 27% when using a 5  $V_{\text{pk-pk}}$  sinusoid. However, when the suspension media was exchanged for HEPES when immobilisation was achieved using a signal operating at 5  $V_{\text{pk-pk}}$  the trapping efficiency increased to 82%. This was conjectured to be attributed to the additional ions present in HEPES compared to LEC.

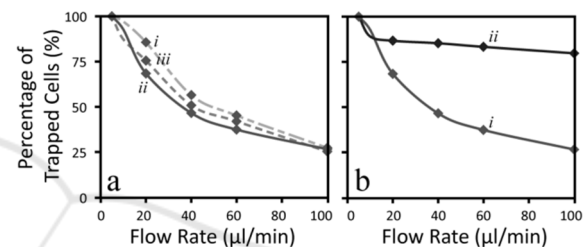


Figure 6: Yeast trapping efficiency analysis (a) Influence of the exciting waveform voltage used during electric field activation, at (i) 2.5, (ii) 5, and, (iii) 10  $V_{\text{pk-pk}}$ . (a) Influence of the medium used after deactivation of the electric field both conducted at an exciting waveform voltage of 5  $V_{\text{pk-pk}}$ , in (i) LEC, and (ii) HEPES.

## 3 APPLICATION

To highlight the functionality of our system, we investigated the response of intracellular calcium signalling of HEK-293-TRPV4 cells to shear induced stress. Shear stress is one of many stimuli that cells respond to, others include, thermal and capsaicin, for example. These stimuli regulate various biological processes, such as proliferation, apoptosis, transcription, and proliferation (Ahern, 2013, Jaalouk and Lammerding, 2009, Polacheck et al., 2013, Lin and Corey, 2005).

HEK-293 cells are transfected to express the TRPV4 (transient receptor potential vanilloid) mechanosensitive ion channel, as HEK-293 cells are limited in the ion channels it expresses. TRPV4 ion channels are of interest as they play a role in controlling vascular homeostasis and tone (Mendoza et al., 2010, Nilius et al., 2004, Baratchi et al., 2014). Furthermore, studies into the influence of shear stress has been restricted as using current methods

for used for HEK-293 cells limits the maximum level of shear induced stress without extensive cell dislodgement.

### 3.1 HEK-293-TRPV4 Cell Preparation

HEK-293 T-REx (Life Sciences) cell lines where prepared off-chip, will full experimentation including viability assays carried out on the microfluidic platform. Firstly, the cells were grown in tetracycline-free DMEM media supplemented 10% FBS, blasticidin (5  $\mu\text{g/ml}$ ) and hygromycin (50  $\mu\text{g/ml}$ ). Secondly, 12 hours before experimentation, the TRP channel expression was induced in the HEK-293 cells using 0.1  $\mu\text{g/ml}$  of tetracycline (Poole et al., 2013). Taking note, that HEK-293 expresses a limited number of TRP channels; thus, making HEK-293 a good candidate to analysis calcium influx through the TRPV4 channel. Additionally, non-transfected HEK-293 T-REx cells were used as a negative control; results not presented here, trapping efficiency was not affected by being non-transfected, additionally no response was observed in the occurrence of shear induced stress.

In the case for investigating shear induced intracellular calcium signalling, the cells required further preparation at the time of experimentation, such that the cells were loaded with Fluo-4AM, and suspended in HEPES-buffered saline solution (140 mM NaCl, 5 mM KCl, 10 mM HEPES, 11 mM D-glucose, 1 mM  $\text{MgCl}_2$ , 2 mM  $\text{CaCl}_2$ , and 2 mM probenecid, adjusted to pH 7.4). After bring incubated at 37 °C for 30 minutes, 25  $\mu\text{l}$  of the HEK-293-TRPV4 cell suspension is suspended in 1000  $\mu\text{l}$  of LEC, making sure not to gently mix the solution, to minimise pre-exposure to shear induced stress.

Additionally, the viability of the cells was examined on-chip with propidium iodide (PI) (10  $\mu\text{g/ml}$ ) staining, at the completion of each experiment.

### 3.2 Experimental Procedure Considerations

Initially cells needed to be characterised on the designed dielectrophoresis platform, such that the Clausius-Mossotti factor response to frequency was investigated. The effect of the technique of discontinuous dielectrophoresis was compared to conventional dielectrophoresis, to highlight the significant improvement on mortality rates of cells. Furthermore, the trapping efficiency was investigated, to ensure that discontinuous

dielectrophoresis was going to be suitable for investigating high shear induced stress. Finally, once the response of HEK-293 cells to discontinuous dielectrophoresis was characterised, shear induced intracellular calcium signalling was investigated, at shear stress levels of 0.875 and 42  $\text{dyn/cm}^2$ .

#### 3.2.1 HEK-293 Clausius-Mossotti Factor

The crossover frequency for HEK-293 cells was examined on chip for three different suspension medium conductivities. Consequently, the measured crossover frequencies were determined to be  $55 \pm 7$ ,  $145 \pm 17$ , and  $285 \pm 45$  MHz, corresponding to conductivities of 200, 500, and 1000  $\mu\text{S/cm}$ , respectively. Conductivities were achieved by adjusting the initial LEC buffer with the addition of PBS. Once the crossover frequencies were obtained, the Clausius-Mossotti factor can be determined for the three conductivities over the frequency range of  $10^4$  to  $10^8$  Hz, as presented in **Figure 7**, taking note the geometric and dielectric properties of HEK-293 cells presented in **Table 2**. Furthermore, the equivalent single shell model is used, as expressed in **Equation 4**, unlike yeast, as HEK-293 cells do not have a cell wall. Such that dielectrophoresis experiments involving HEK-293 cells, were conducted using a conductivity of 200  $\mu\text{S/cm}$ , using an operating frequency of 10 MHz, which is well within the positive dielectrophoresis range (**Figure 7a**). Additionally, the combined use of this medium conductivity and operating frequency minimised the manifestation of electrothermal effects, such as vortices and electrolysis.

Table 2: Geometric and dielectric properties of viable HEK-293 cells used to determine dielectrophoresis behaviour (Soffe et al., 2015a).

Parameter	Value
Cell diameter	12.5 $\mu\text{m}$
Membrane thickness	7 nm
Cytoplasm conductivity	0.5 S/m
Cytoplasm permittivity	$60\epsilon_0$ F/m
Membrane conductivity	$7\text{e-}14$ S/m
Membrane permittivity	$9.5\epsilon_0$ F/m

#### 3.2.2 HEK-293 Cell Viability

Viability assays for HEK-293 were conducted under three different environmental scenarios, for a period of 60 minutes, with the microelectrodes excited with a 10 MHz sinusoid operating at 5  $V_{\text{pk-pk}}$  (**Figure 8**). Viability assays were limited to 60 minutes, as the longest duration for a shear stress experiment was 30

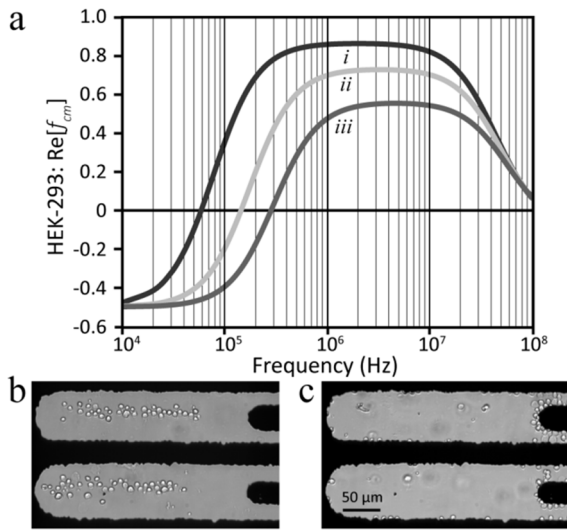


Figure 7: (a) The real part of Clausius-Mossotti factor response to frequency for HEK-293 cells at medium conductivities of (i) 200, (ii) 500, and (iii) 1000  $\mu\text{S/cm}$ . Conductivities were achieved by adjusting the initial LEC buffer with the addition of PBS Experimental images of (b) positive; and (c) negative dielectrophoresis; taken when determining the crossover frequency for HEK-293 cells.

minutes, so 60 minutes should suffice. Cell viability was determined by evaluating, the following equation:

$$n_{\text{cell viability}} = \frac{n_{\text{remaining viable}}}{n_{\text{initial viable}}} \cdot 100\%, \quad (14)$$

where,  $n_{\text{remaining viable}}$ , and  $n_{\text{initial viable}}$  are the number of remaining and initial cell counts of viable cells. Non-viable cells were determined through PI staining, and excluded from the viable cell count.

Scenario one (Figure 8i), conventional dielectrophoresis, such that the cells are suspended in LEC and the electric field is activated for the entire 60 minutes and two additional minutes to be comparable to the other two scenarios. In scenario two (Figure 8ii), the electric field was activated for a period of 120 s, and the cells are suspended in LEC. In scenario three (Figure 8iii), the electric field was activated for a period of 120 s, and the cells are suspended in HEPES once the field is deactivated.

The viability assays indicated that the continued presence of the electric field (Scenario one) significantly affects the viability of cells, such that 88% of cells are viable. However, the viability percentage is significantly increased when discontinuous dielectrophoresis is invoked; such that approximately 98% of the cells are viable regardless

of cell suspension. Although cells suspended in HEPES have a slightly higher viability rate (Scenario Three).

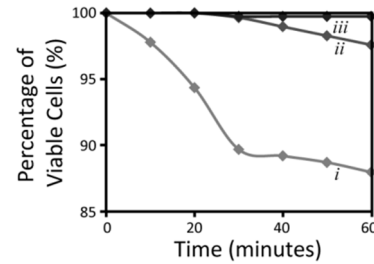


Figure 8: HEK-293-TRPV4 cell viability analysis using PI; conducted using three different scenarios: (i) Conventional dielectrophoresis with cells suspended in LEC (constant electric field activation); (ii) Discontinuous dielectrophoresis with cells suspended in LEC; and (iii) Discontinuous dielectrophoresis with cells suspended in HEPES.

### 3.2.3 HEK-293 Trapping Efficiency

A more extensive trapping efficiency analysis was carried out for HEK-293, due to the cell being more susceptible to environmental influences, such as: the supplied waveform parameters during electric field application; and the suspension media, which assists in regulating cellular behaviour. The influence of the exciting waveform was examined, using three different voltages, being 2.5, 5, and 10  $V_{\text{pk-pk}}$  for three different scenarios (Figure 9a-c), with the trapping efficiency determined using Equation 13. In scenario one (Figure 9a), conventional dielectrophoresis, a supply voltage of 5  $V_{\text{pk-pk}}$  produced the most effective trapping efficiency of 94%. However, in scenario two (Figure 9b), discontinuous dielectrophoresis was invoked, with the cells suspended in LEC, all initially immobilised cells were dislodged at a flow rate of 100  $\mu\text{l/min}$  (35  $\text{dyn/cm}^2$ ). Furthermore, in scenario three (Figure 9c), discontinuous dielectrophoresis was invoked, with the cells suspended in HEPES. In this scenario, the percentage of immobilised cells significantly increased, regardless of the supplied voltage, to a trapping efficiency between 84% and 90%. In comparison to scenario two, this indicated that the presence of a biologically relevant media, is crucial in ensuring cells remain immobilised.

Optimal conditions presented in Figure 9d, the three aforementioned scenarios, are displayed for a supply voltage of 5  $V_{\text{pk-pk}}$  (Figure 9di-iv). Additionally, a control comparison was conducted (Figure 9di), achieved by allowing cells suspended



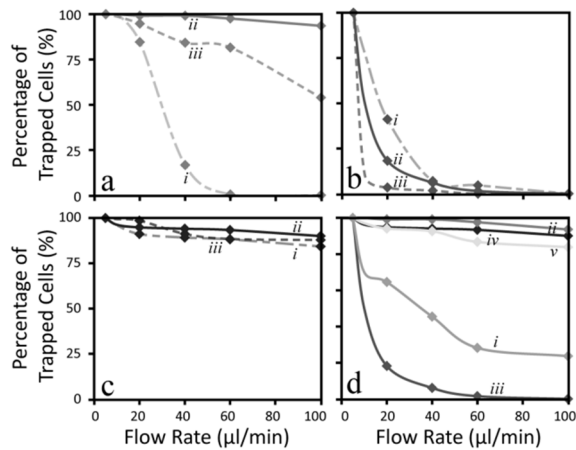


Figure 9: Trapping efficiency of HEK-293-TRPV4 under different environmental scenarios. For (a) Conventional dielectrophoresis with cells suspended in LEC (constant electric field activation); (b) Discontinuous dielectrophoresis with cells suspended in LEC; and (c) Discontinuous dielectrophoresis with cells suspended in HEPES. Furthermore, for each scenario the exciting waveform voltage used during electric field activation was examined at (i) 2.5, (ii) 5, and (iii) 10  $V_{pk-pk}$ . (d) Conducted under different environmental scenarios in optimal conditions (supplying sinusoid waveform operating at 10 MHz 5  $V_{pk-pk}$ ): (i) Control, with no dielectrophoresis with cells suspended in HEPES; (ii) Conventional dielectrophoresis with cells suspended in LEC; (iii) Discontinuous dielectrophoresis with cells suspended in LEC; (iv) Discontinuous dielectrophoresis with cells suspended in HEPES; and (v) Discontinuous dielectrophoresis with cells suspended in HEPES using a PDMS substrate instead of a glass substrate.

in HEPES to rest on the non-treated glass substrate for 30 minutes; thus, simulating cells being immobilised by dielectrophoresis. At a flow rate of 100  $\mu\text{l}/\text{min}$ , equivalent to 35  $\text{dyn}/\text{cm}^2$ , the control experiments led to a trapping efficiency of 24%, which was a significant improvement of cells suspended in LEC using discontinuous dielectrophoresis (scenario two), in which case all the cells were dislodged. However, cells either trapped using conventional dielectrophoresis or discontinuous dielectrophoresis with cells suspended in HEPES, resulted in the optimal trapping efficiencies.

An additional comparison was made to examine the importance of the substrate, such that discontinuous dielectrophoresis was invoked, using a platform with microelectrodes fabricated on PDMS on glass substrate (Figure 9d<sub>v</sub>) (Nasabi et al., 2013). These results indicated that, discontinuous dielectrophoresis when using a biological relevant media is produces the highest

trapping efficiency, when applying high shear stresses, such as 35  $\text{dyn}/\text{cm}^2$  (100  $\mu\text{l}/\text{min}$ ).

Although, the application of conventional dielectrophoresis using a supply voltage of 5  $V_{pk-pk}$ , resulted in the highest trapping efficiency (93%), the continued electric field application affected cell viability as presented in Figure 8. Thus, conventional dielectrophoresis was determined not suitable for shear stress analysis of HEK-293 cells. On the other hand, discontinuous dielectrophoresis, with a slightly lower trapping efficiency of 90%, minimised effects on cell viability (Figure 8), and enabled experimentation to be carried out in a biologically relevant media (HEPES).

### 3.3 Intracellular Calcium Signalling Analysis of HEK-293-TRPV4

Intracellular calcium signalling is important as it facilitates in the regulation of several biological processes. The calcium ion ( $\text{Ca}^{2+}$ ) is of importance, as it regulates a variety of spatial and temporal signals. The movement of calcium ions is facilitated through the stimulation of permeable ion channels, such as the TRPV4 ion channel. The influx of calcium ions through calcium permeable ion channel into the plasma membrane, occurs due an induced stimulation of their selective stimulus, such as shear stress a form of mechanical stimulation (Mendoza et al., 2010, Baratchi et al., 2014). The level of intracellular calcium level ( $[\text{Ca}^{2+}]_i$ ), due to calcium influx is measured through the use of calcium sensitive dyes.

A comparison was undertaken of the influence of shear stress on the behaviour of intracellular calcium influx, using HEK-293 cells expressing TRPV4. Cells were prepared off-chip with Fluo-4AM, a calcium sensitive dye, as outlined previously. Intensity measurements were then acquired using an inverted microscope, equipped with a photomultiplier tube, a near infrared camera (QuantEM:512SC, Photometrics), and a 10 $\times$  objective (CFI Plan Apo Lambda 10 $\times$ ). With the assistance of NIS Elements, microscope imaging software (Basic Research, Nikon Instruments), the intensity measurements were able to be processed.

Intracellular calcium signalling analysis was then carried out using discontinuous dielectrophoresis with cells suspended in HEPES, with the microelectrodes excited with a 10 MHz sinusoid operating at 5  $V_{pk-pk}$ . The influence of shear stress on intracellular calcium signalling through the TRPV4 ion channel, was conducted by subjecting immobilised cells to shear stress for a period of

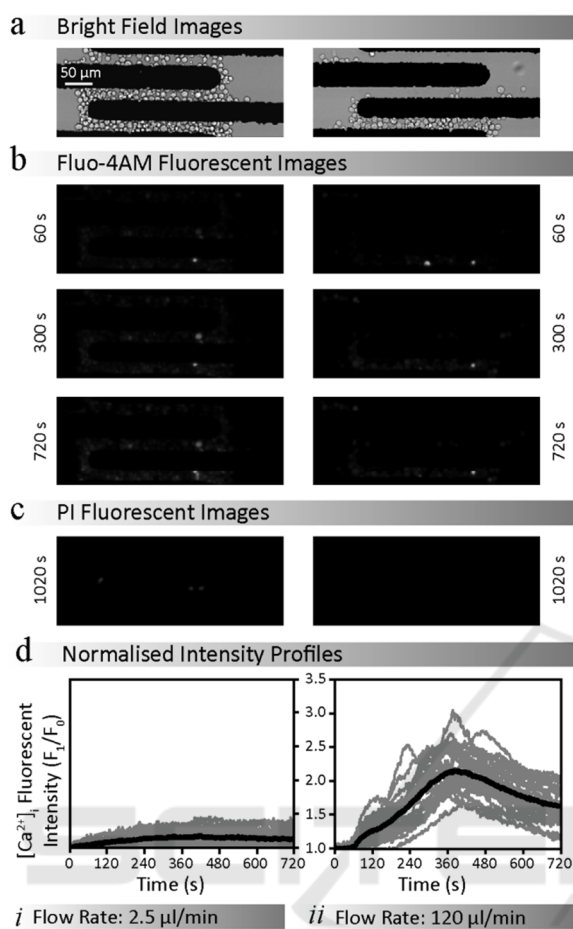


Figure 10: HEK-293-TRPV4 cell response to shear stress achieved using flow rates of (i) 2.5, and (ii) 120 μl/min. With the retrospective images of the immobilised cells in: (a) Bright field; (b) Fluorescent images of cells loaded with Fluo-4AM obtained at 60, 300, and 720 s; and (c) PI fluorescent images taken at 1020 s; 300 s after the addition of PI to the microfluidic platform. (d) Corresponding normalised intensity profile over period of 720 s.

720 s, and measuring the intensity of the calcium dye (Fluo-4AM) (Figure 10). A shear stress of 42 dyn/cm<sup>2</sup> (120 μl/min), was selected, as this shear stress is in the upper region of the physiological shear stress range (Figure 10ii); consequently, highlighting the capability of discontinuous dielectrophoresis of cells remaining immobilised under high levels of shear stress. The resulting intensity profiles were compared against a negligible shear stress of 0.875 dyn/cm<sup>2</sup> (2.5 μl/min), to maintain the cells with a fresh supply of HEPES (Figure 10i).

A shear stress level of 42 dyn/cm<sup>2</sup> resulted in a percentage of activated cells of 73.1 ± 12.5%, and maximum fold increase in  $[Ca^{2+}]_i$  of 2.27 ± 0.07. In

comparison to negligible shear stress (0.875 dyn/cm<sup>2</sup>), which resulted in a percentage of activated cells of 3.25 ± 1.2%, and a maximum fold increase in  $[Ca^{2+}]_i$  of 1.17 ± 0.09. Furthermore, a decrease in the cellular and peak response times was observed with the higher shear stress level. Such that the cellular response time decreased from 130 ± 40 s to 77 ± 6 s, and the peak response time decreased from 426 ± 36 s to 392 ± 18 s, for shear stress levels of 0.875, and 42 dyn/cm<sup>2</sup>, respectively. Consequently, indicating that the calcium influx intensifies with higher shear stress levels, and the importance of being able to investigate high shear stress on a cellular physiological level.

## 4 CONCLUSIONS

Discontinuous dielectrophoresis provides a strategy for analysing the response of loosely adherent cells to high levels of shear stress. We have demonstrated procedure of discontinuous dielectrophoresis using *S. cerevisiae* yeast cells, and the capacity of the immobilised cells to withstand high levels of shear stress. We then in turn, investigated the capability of the system using HEK-293 cells, a commonly used cell line for biological assays. The experimental considerations were investigated for using HEK-293 cells for discontinuous dielectrophoresis, such as: Clausius-Mossotti factor response to frequency; viability and trapping efficiency comparison of conventional and discontinuous dielectrophoresis for cells suspended in LEC or HEPES. For cells immobilised using discontinuous dielectrophoresis, using HEPES as the suspension media after electric field deactivation, resulted in a trapping efficiency of 90% when experiencing a shear stress level of 42 dyn/cm<sup>2</sup>. Additionally, discontinuous dielectrophoresis minimises cell mortality rates, such that after a period of 60 minutes, approximately 98% of cells were deemed viable, through propidium iodide staining.

The capacity of the system for biological analysis under high shear stress was then demonstrated, for investigating the influence of shear stress on intracellular calcium signalling of HEK-293-TRPV4 cells; which indicated the shear stress intensifies the calcium influx. This technique has the ability for investigating various cell responses to high levels of shear stress, as presented here and demonstrated for HEK-293-TRPV4 cells. Furthermore, the platform offers the potential of parallelism, and dynamic analysis through changing the microenvironment within the microchannel, such

as thermal stimuli, in the presence of high shear stress.

## ACKNOWLEDGEMENTS

Khashayar Khoshmanesh acknowledges the Australian Research Council for funding, under the Discovery Early Career Researcher Award (DECRA) scheme, (project DE120101402).

## REFERENCES

- Ahern, G. P. 2013. Transient receptor potential channels and energy homeostasis. *Trends in Endocrinology & Metabolism*, 24, 554-560.
- Baratchi, S., Tovar-Lopez, F. J., Khoshmanesh, K., Grace, M. S., Darby, W., Almazi, J., Mitchell, A. & McIntyre, P. 2014. Examination of the role of transient receptor potential vanilloid type 4 in endothelial responses to shear forces. *Biomicrofluidics*, 8, 044117(1-13).
- Berthier, E., Young, E. W. K. & Beebe, D. 2012. Engineers are from PDMS-land, Biologists are from Polystyrenia. *Lab on a Chip*, 12, 1224-1237.
- Ding, X., Lin, S. C., Kiraly, B., Yue, H., Li, S., Chiang, I. K., Shi, J., Benkovic, S. J. & Huang, T. J. 2012. On-chip manipulation of single microparticles, cells, and organisms using surface acoustic waves. *Proceedings of the National Academy of Sciences*, 109, 11105-9.
- El-Ali, J., Sorger, P. K. & Jensen, K. F. 2006. Cells on chips. *Nature*, 442, 403-411.
- Huang, Y., Holzel, R., Pethig, R. & Xiao, B. W. 1992. Differences in the AC electrodynamics of viable and non-viable yeast cells determined through combined dielectrophoresis and electrorotation studies. *Physics in Medicine and Biology*, 37, 1499.
- Jaalouk, D. E. & Lammerding, J. 2009. Mechanotransduction gone awry. *Nature reviews Molecular cell biology*, 10, 63-73.
- Lin, S.-Y. & Corey, D. P. 2005. TRP channels in mechanosensation. *Current opinion in neurobiology*, 15, 350-357.
- Mendoza, S. A., Fang, J., Gutterman, D. D., Wilcox, D. A., Bubolz, A. H., Li, R., Suzuki, M. & Zhang, D. X. 2010. TRPV4-mediated endothelial Ca<sup>2+</sup> influx and vasodilation in response to shear stress. *American Journal of Physiology-Heart and Circulatory Physiology*, 298, H466-H476.
- Morgan, H. & Green, N. 2003. AC electrokinetics: colloids and nanoparticles. Baldock, England: Research Studies Press Ltd.
- Mutreja, I., Woodfield, T. B. F., Sperling, S., Nock, V., Evans, J. J. & Alkai, M. M. 2015. Positive and negative bioimprinted polymeric substrates: new platforms for cell culture. *Biofabrication*, 7, 025002.
- Nahavandi, S., Tang, S.-Y., Baratchi, S., Soffe, R., Nahavandi, S., Kalantar-Zadeh, K., Mitchell, A. & Khoshmanesh, K. 2014. Microfluidic Platforms for the Investigation of Intercellular Signalling Mechanisms. *Small*, 10, 4810-4826.
- Nasabi, M., Khoshmanesh, K., Tovar-Lopez, F. J., Kalantar-Zadeh, K. & Mitchell, A. 2013. Dielectrophoresis with 3D microelectrodes fabricated by surface tension assisted lithography. *ELECTROPHORESIS*, 34, 3150-3154.
- Nilius, B., Vriens, J., Prenen, J., Droogmans, G. & Voets, T. 2004. TRPV4 calcium entry channel: a paradigm for gating diversity. *American Journal of Physiology-Cell Physiology*, 286, C195-C205.
- Polacheck, W. J., Li, R., Uzel, S. G. & Kamm, R. D. 2013. Microfluidic platforms for mechanobiology. *Lab on a Chip*, 13, 2252-2267.
- Poole, D. P., Amadesi, S., Veldhuis, N. A., Abogadie, F. C., Lieu, T., Darby, W., Liedtke, W., Lew, M. J., McIntyre, P. & Bunnett, N. W. 2013. Protease-activated Receptor 2 (PAR(2)) Protein and Transient Receptor Potential Vanilloid 4 (TRPV4) Protein Coupling Is Required for Sustained Inflammatory Signaling. *Journal of Biological Chemistry*, 288, 5790-5802.
- Soffe, R., Baratchi, S., Tang, S.-Y., Nasabi, M., McIntyre, P., Mitchell, A. & Khoshmanesh, K. 2015a. Analysing the calcium signalling of cells under high shear flows using discontinuous dielectrophoresis. *Scientific Reports*, 5, 11973.
- Soffe, R., Tang, S.-Y., Baratchi, S., Nahavandi, S., Nasabi, M., Cooper, J. M., Mitchell, A. & Khoshmanesh, K. 2015b. Controlled Rotation and Vibration of Patterned Cell Clusters Using Dielectrophoresis. *Analytical Chemistry*, 87, 2389-2395.
- Urdaneta, M. & Smela, E. 2007. Multiple frequency dielectrophoresis. *ELECTROPHORESIS*, 28, 3145-3155.
- Voldman, J. 2006. Engineered systems for the physical manipulation of single cells. *Current opinion in biotechnology*, 17, 532-537.
- Whitesides, G. M., Ostuni, E., Takayama, S., Jiang, X. & Ingber, D. E. 2001. SOFT LITHOGRAPHY IN BIOLOGY AND BIOCHEMISTRY. *Annual Review of Biomedical Engineering*, 3, 335-373.
- Yamamoto, K. & Ando, J. 2013. Endothelial cell and model membranes respond to shear stress by rapidly decreasing the order of their lipid phases. *Journal of cell science*, 126, 1227-1234.
- Yamamoto, T. & Fujii, T. 2007. Active immobilization of biomolecules on a hybrid three-dimensional nanoelectrode by dielectrophoresis for single-biomolecule study. *Nanotechnology*, 18, 495503.